International Journal of Heat and Mass Transfer 52 (2009) 1774–1777

Contents lists available at ScienceDirect

International Journal of Heat and Mass Transfer

journal homepage: www.elsevier.com/locate/ijhmt

Kinetics of water adsorption/desorption under isobaric stages of adsorption heat transformers: The effect of isobar shape

I.S. Glaznev [a], D.S. Ovoshchnikov [a,b], Yu.I. Aristov [a,*]

[a] Boreskov Institute of Catalysis, Pr.Lavrentieva, 5, Novosibirsk 630090, Russia
[b] Novosibirsk State University, Pirogova st. 2, Novosibirsk 630090, Russia

ARTICLE INFO

Article history:
Received 8 July 2008
Received in revised form 25 August 2008
Available online 6 December 2008

Keywords:
Adsorption/desorption rate
Adsorption heat transformer
Selective water sorbent
Dynamic optimization
Isobar shape

ABSTRACT

Effect of the shape of equilibrium adsorption isobar on dynamics of water adsorption/desorption under isobaric stages of a basic cycle of an adsorption heat transformer has been studied. Selective water sorbent SWS-1L ($CaCl_2$ confined to mesoporous silica gel) was used for these tests as its water adsorption isobars have segments with both convex and concave shapes. From these experiments the conclusion has been drawn that the dynamics of adsorption on a single adsorbent grain is closely linked with the shape (convex or concave) of the segment of water adsorption isobar between initial and final temperatures of the isobaric process. In particular, under the same boundary conditions desorption is faster than adsorption for a concave isobar segment and vice versa for a convex one.

1. Introduction

An adsorbent is a key element of an adsorptive heat transformer, AHT (heat pump, chiller and amplifier), and its proper choice is of prime importance [1–3]. Thermodynamic requirements to an optimal adsorbent which ensures the best cycle performance under prescribed operating conditions were reported for non-regenerative AHT cycles in [4–5]. Kinetic properties of the adsorbent strongly affect the dynamic behavior of AHT and contribute to the specific power of the unit. Hence, it is important to specify what should be an optimal adsorbent for AHT from dynamic point of view. It is a quite complicated task as many parameters can affect the dynamic behavior of AHT. Among them are common thermo-physical and structural parameters, such as a size of the pores (voids) which serve for transport of a working fluid to adsorption centers, a heat conductivity of the adsorbent skeleton that ensures the heat transfer in the grain, grain porosity, pores interconnection, grain size, etc. [6–8].

More sophisticated interplay between the dynamic and thermodynamic properties of the adsorbent for AHT was predicted in [9]. In that paper a detailed mathematical model of the adsorption/desorption process was developed for detailed analysis of temporal evolution of the radial distributions of water uptake, vapor pressure inside the grain and grain temperature (as well as their average values). The model was developed for describing the coupled heat and mass transfers in the case when the adsorption on single grain is initiated by a fast change in the temperature of metal plate under the grain. It was used to analyze the experiments on water adsorption dynamics on loose grains of composite adsorbent "$CaCl_2$/silica KSK" presented in [10]. The adsorption was initiated by temperature jump (drop) similar to that commonly realized in AHT, e.g., from 60 down to 35 °C during adsorption stage and from 60 to 90 °C during desorption stage. Reverse jumps have also been performed to compare the adsorption and desorption dynamics under the same boundary conditions. The vapor pressure during these measurements was maintained almost constant, that allowed a close imitation of the isobaric stages of basic AHT cycle [10].

The modeling predicted that the dynamics of water adsorption on a single adsorbent grain is closely linked with equilibrium properties of the adsorbent, in particular, with the initial/final temperatures and with the shape of the segment of water sorption isobar (linear, convex or concave) between these temperatures. In particular, the model forecasted that under the same boundary conditions (e.g., a temperature jump from 60 to 90 °C and back) the desorption is faster than adsorption for a concave isobar and vice versa for a convex one, while for linear isobar the kinetic curves coincide [9]. The aim of the present paper is an experimental validation of this hypothesis. The composite adsorbent SWS-1L [11] was used for these tests as its water adsorption isobars have segments with both convex and concave shapes (Fig. 1). It allowed careful measurements of adsorption/desorption dynamics for the both cases, as well as a qualitative comparison with the model predictions [10].

* Corresponding author. Tel./fax: +7 383 330 9573.
E-mail address: aristov@catalysis.ru (Yu.I. Aristov).

0017-9310/$ - see front matter © 2008 Elsevier Ltd. All rights reserved.
doi:10.1016/j.ijheatmasstransfer.2008.09.031

Nomenclature

AHT	adsorption heat transformer (−)
J	heat flow (wt/m^2)
N	amount of adsorbed water per 1 mole of $CaCl_2$ (mol/mol)
P_{H_2O}	pressure of water vapor (mbar)
S	contact surface between the fins and the adsorbent (m^2)
t	time (s)
T	temperature (K)
T_{ads}	minimal temperature of adsorption of AHT cycle (K)
T_{des}	minimal temperature of desorption of AHT cycle (K)
V	valve (−)
V_{MC}	volume of measuring cell (m^3)
V_{VV}	volume of vapor vessel (m^3)
3WV	three-way valve (−)
w	water uptake of adsorbed water (kg/kg)

Greek symbols

α	coefficient of heat transfer (W/m^2 K)
Δ	difference operator (−)
χ	dimensionless differential water loading

Subscripts

0	initial value at $t = 0$
c	condenser
e	evaporator
g	generator
f	final value

2. Experimental apparatus, procedure and materials

We used the experimental setup described elsewhere [12]. It contained two main compartments: the measuring cell (volume $V_{MC} = 0.14 \times 10^{-3}$ m^3) and the vapor vessel ($V_{VV} = 30.5 \times 10^{-3}$ m^3) (Fig. 2). The absolute pressure transducer MKS Baratron® type 626A (accuracy ± 0.01 mbar) was used to control the pressure. Loose adsorbent grains were placed on an isothermal surface of the metal holder. Its temperature can be adjusted with the accuracy of ±0.1 °C using a heat carrier circuit coupled by a three-way valve (3WV) either to circulating thermal bath 1 or 2 (Fig. 2).

The experimental setup was evacuated and filled with water vapor. By rotating the 3WV to the reverse position, the heat carrier flows from bath 1 and bath 2 could be switched and, thus, initiating either adsorption or desorption process. It resulted in reducing/increasing the vapor pressure over the adsorbent, which did not exceed 2.0–2.5 mbar, so that the process could be considered as quasi-isobaric. The water uptake $w(t)$ was calculated from the temporal pressure evolution $P_{H2O}(t)$ as described in [10]. Two adsorption/desorption runs have been performed (Fig. 1). The first adsorption/desorption run was carried out between point 2 (T = 60 °C) and point 1 (T = 35 °C) with a concave shape of the curve w(T) (Fig. 1). The second adsorption/desorption run was performed between point 2′ (T = 60 °C) and point 3 (T = 90 °C). The latter segment has a convex shape.

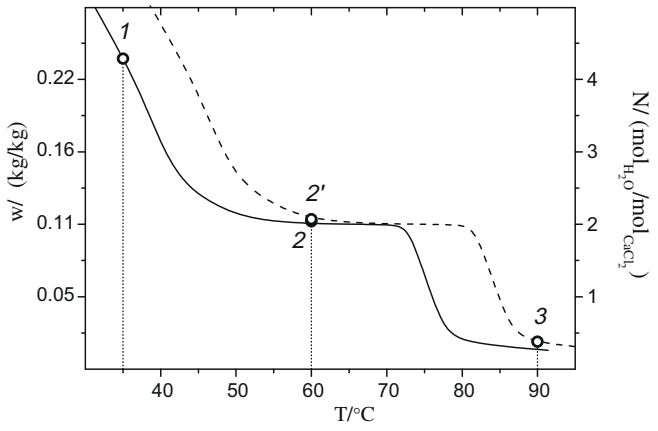

Fig. 1. Water sorption isobars of "SWS-1L – H_2O": 7.8 mbar (solid line) and 12.2 mbar (dashed line). The initial and final values of temperature jumps are remarked by points 1 – 35 °C; 2, 2′ – 60 °C; 3 – 90 °C.

The tested adsorbent SWS-1L was prepared by a dry impregnation of a silica KSK with a saturated aqueous solution of $CaCl_2$ at T = 25 °C. The synthesis procedure was described in [11]. The salt content amounted to 33.7 wt% (dry base). The grain size was selected between 1.4 and 1.6 mm.

3. Results and discussion

After initiating the holder cooling/heating, its temperature reached the final temperature T_f within app. 1 min, while the pressure reduction/increasing was much slower and completed within some 10 min (Fig. 3). For the first minute (the dimensionless uptake $\chi \leqslant 0.1$) the sorption dynamics was almost identical for all uptake curves, probably because it was determined mainly by the rate of heating/cooling of the metal holder. At longer times the kinetic curves become different, and the desorption rate was faster than the adsorption for segment 1–2 (Fig. 3a) and slower for segment 2′–3 (Fig. 3b) that was in complete agreement with calculations reported in [9].

The qualitative explanation of such behavior can be done by considering a coupled heat and mass transfer in the system "adsorbent grain-metal plate". For jump 60 °C ⇒ 35 °C at the beginning of adsorption process ($t \approx 0$) (point 2) the driving force for heat transfer is maximum because the plate is already cold ($T \approx 35$ °C) while the adsorbent grain is still at $T \approx 60$ °C. Although the conditions for removing adsorption heat are optimal, almost no heat is transferred from the grain to the holder because at point 2 the derivative dw/dT is close to zero, hence, the adsorbed amount is rather small. On the contrary, when approaching point 1 the temperature difference between the plate and the grain is getting smaller and smaller, while the amount of the adsorption heat to be removed is increasing replicating the gradual rise of the derivative dw/dT. This discordance between the heat removal and heat release results in significant deceleration of the adsorption process and very slow reaching the adsorption equilibrium at long times (Fig. 3a).

Much better correlation takes place during the reverse desorption process 35 °C ⇒ 60 °C (from point 1 to point 2, Fig. 1). Indeed, in this case the derivative dw/dT and, hence, the heat supply requested for water desorption are maximum at $t = 0$ when the conditions of heat transfer from the metal to the grain are the most favorable as well. This is the main reason why for a concave shape of the curve $w(T)$ the adsorption process is always slower than the desorption one as it was observed in [10] and confirmed by calculations in [9]. Experimental testing of adsorption/desorption

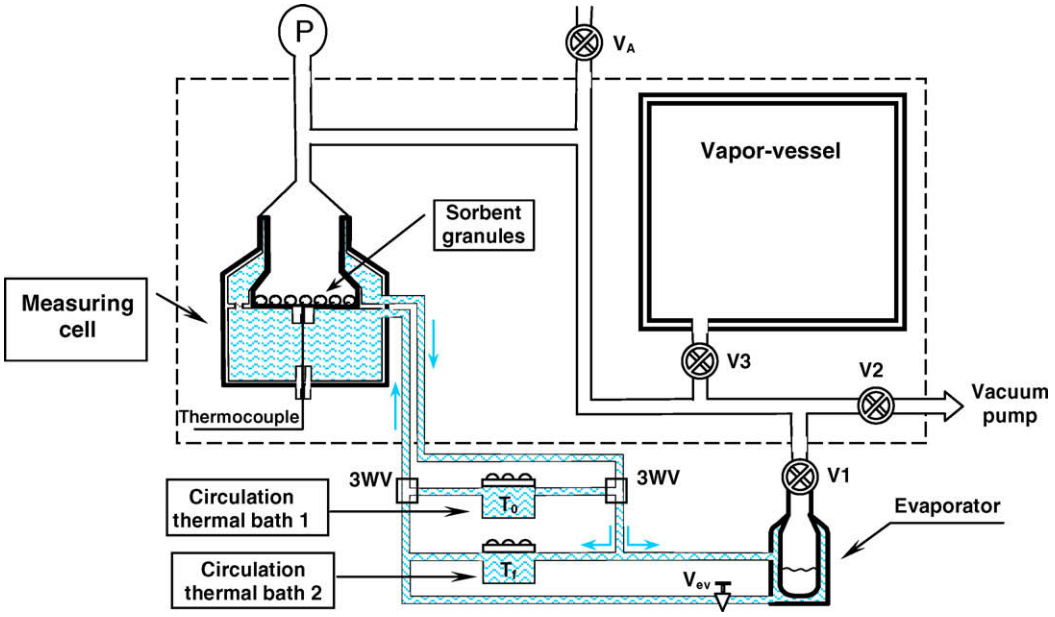

Fig. 2. Schematic diagram of the kinetic setup.

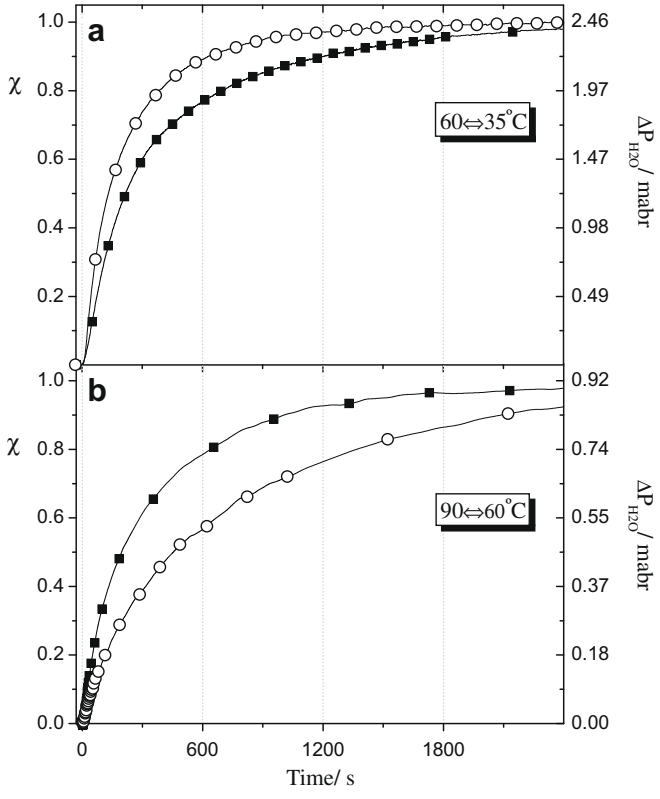

Fig. 3. Experimental kinetic curves of water adsorption (solid squares) and desorption (open circles) for SWS-1L grains at different temperature jumps: (a) 60 ⟺ 35 °C, points 2 ⟺ 1; (b) 60 ⟺ 90 °C, points 2′ ⟺ 3 (Fig. 1).

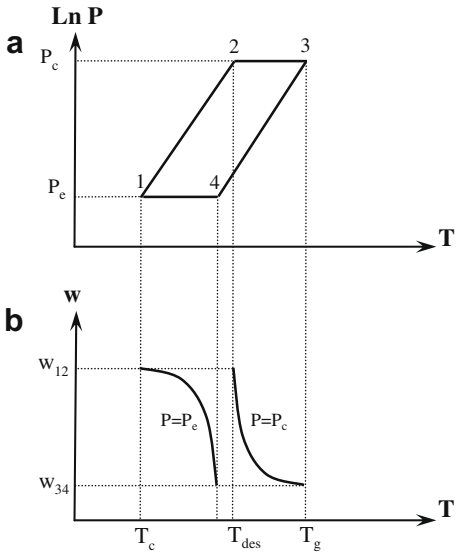

Fig. 4. Basic AHT cycle (a) and dynamically optimal isobar shape (b).

kinetics for a convex segment of the water adsorption isobar was performed in this paper (between points 2′ and 3, Fig. 1). These tests (Fig. 3b) unambiguously proved the predictions done in [9], because in this case the mentioned discordance of the heat fluxes was observed during the desorption process which appeared to be more slow than the adsorption one (Fig. 3b).

Thus, a correlation between the driving force for heat transfer and the derivative dw/dT which defines the heat demand for desorption or heat release during adsorption, is dominant for overall adsorption dynamics in real AHT. Since this driving force is gradually reducing, the derivative should decrease when T is approaching the final temperature T_f, too. Hence, d^2w/dT^2 has to be negative. It means that to shorten the isobaric stages, at desorption run the isobar has to be concave while at adsorption run – convex (Fig. 4). For common adsorbents (silicas, zeolites, etc.) this situation looks unrealistic because adsorption isobars at various pressures usually have a concave shape, the sign of the derivative d^2w/dT^2 is positive and does not change with w. Such shape is favorable for desorption stage and unfavorable for adsorption stage; thus, the latter is commonly longer. However, adsorbents with S-shaped adsorption isobars (SWSs, FAMs, porous carbons, etc.) have both convex and concave segments and appropriated optimization may, in principle, be done by a proper choice of the segment.

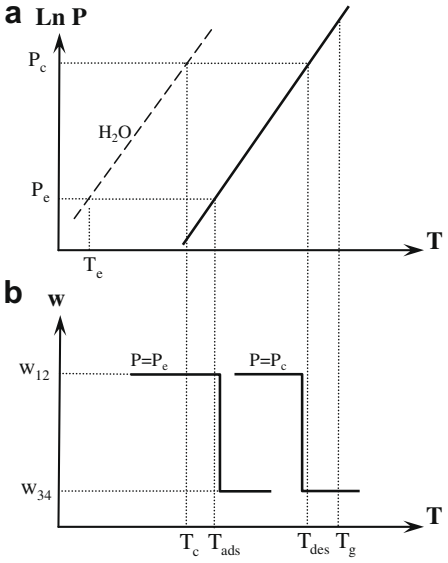

Fig. 5. Confluent AHT cycle (a) with a step-like adsorption isobars (b).

This analysis shows that for the process intensification and reduction of the cycle time the most profitable is to supply the majority of heat to or reject it from the adsorbent layer at maximal acceptable temperature difference between the metal and the adsorbent. In our opinion, the most challenging shape of adsorption isobar is a step-like isobar (Fig. 5). At desorption stage, the position of isobar step should be close to the minimum desorption temperature T_{des} (defined in [13]), while the generator temperature T_g should be higher to create sufficient driving force for supplying heat for desorption. At adsorption stage the step should be positioned at temperature T_{ads} that is higher than the temperature T_c of cooling fluid to create sufficient driving force for rejecting heat of adsorption. Due to this specific shape of adsorption isobar the temperature difference between adsorbent layer and metal plate will remain almost constant $T_g - T_{des}$ (or $T_{ads} - T_c$) during the dehydration (or hydration) and will quickly reduce to zero as soon as the process is completed. Thus, during the adsorption the heat flux from the adsorbent layer to the cooling fluid is almost constant and can be estimated (in the absence of diffusional resistances) as $J = \alpha S(T_{ads} - T_c)$, where α is a coefficient of heat transfer between metal fins and adsorbent, S is the contact surface between the fins and the adsorbent.

It is worthy to mention that the dynamic requirement to maximize the temperature difference $T_g - T_{des}$ (or $T_{ads} - T_c$) is in a distinct contradiction with the thermodynamic requirements specified in [4,5]. Indeed, it is evident that from thermodynamic point of view it is quite favorable to minimize both the differences $(T_g - T_{des})$ and $(T_{ads} - T_c)$ to reduce the entropy generation during isobaric stages of AHP cycle. Reasonable compromise can be reached by increasing either α or/and S that is a subject of intelligent designing the system "adsorbent-heat exchanger".

4. Conclusions

From the experiments performed the conclusion has been drawn that dynamics of water adsorption on a single adsorbent grain is closely linked with the shape (convex or concave) of the segment of water adsorption isobar between the initial and final temperatures. In particular, under the same boundary conditions desorption is faster than adsorption for a concave isobar segment and vice versa for a convex one. We proposed that the most challenging shape of adsorption isobar is a step-like isobar. It ensures a constant temperature difference between the adsorbent and heat exchanger fins during isobaric adsorption and desorption stages, and, hence, the maximal rate of heat transfer to (from) the adsorbent layer. In the absence of inter- and intra-particle diffusional resistances this will maximize the adsorption (desorption) rate and cooling (heating) power of AHT.

Acknowledgments

The authors thank the Russian Foundation for Basic Researches (projects 08-08-00808, 03-05-34762 and 08-08-90016) for partial financial support.

References

[1] N.C. Srivastava, I.W. Eames, A review of adsorbents and adsorbates in solid-vapor adsorption heat pump systems, Appl. Therm. Eng. 18 (1998) 707–714.
[2] F.P. Schmidt, J. Luther, E.D. Glandt, Influence of adsorbent characteristics on the performance of an adsorption heat storage cycle, Ind. Eng. Chem. Res. 42 (2003) 4910–4918.
[3] R. Critoph, Y. Zhong, Review of trends in solid sorption refrigeration and heat pumping technology, Proc. Inst. Mech. Eng. E: J. Process Mech. Eng. 219 (2005) 285–300.
[4] Yu.I. Aristov, An optimal sorbent for adsorption heat pumps: thermodynamic requirements and molecular design, in: Proc. VI Int. Seminar "Heat Pipes, Heat Pumps, Refrigerators", Belarus, 2005, pp. 342–353.
[5] Yu.I. Aristov, Novel materials for adsorptive heat pumping and storage: screening and nanotailoring of sorption properties, J. Chem. Eng. Jpn. 40 (13) (2007) 1241–1251.
[6] D. Ruthven, Principles of Adsorption and Adsorption Processes, John Wiley and Sons, Inc., New York, USA, 1984.
[7] A. Sakoda, M. Suzuki, Simultaneous transport of heat and adsorbate in closed type adsorption cooling system utilizing solar heat, ASME J. Solar Energy Eng. 108 (2) (1986) 239–245.
[8] B.B. Saha, E.C. Boelman, T. Kashiwagi, Computational analysis of an advanced adsorption–refrigeration cycle, Energy 20 (1995) 983–994.
[9] B.N. Okunev, A.P. Gromov, L.I. Heifets, Yu.I. Aristov, A new methodology of studying the dynamics of water vapor sorption/desorption under real operating conditions of adsorption heat pumps: modeling of coupled heat and mass transfer in a single adsorbent grain, Int. J. Heat Mass Transfer 51 (2008) 246–252.
[10] Yu.I. Aristov, B. Dawoud, I.S. Glaznev, A. Elyas, A new methodology of studying the dynamics of water vapor sorption/desorption under real operating conditions of adsorption heat pumps: experiment, Int. J. Heat Mass Transfer 51 (2008) 4966–4972.
[11] Yu.I. Aristov, M.M. Tokarev, G. Cacciola, G. Restuccia, Selective water sorbents for multiple applications: 1. $CaCl_2$ confined in mesopores of the silica gel: sorption properties, React. Kinet. Catal. Lett. 59 (2) (1996) 325–334.
[12] I.S. Glaznev, Yu.I. Aristov, Kinetics of water adsorption on loose grains of SWS-1L under isobaric stages of adsorption heat pumps: the effect of residual air, Int. J. Heat Mass Transfer 51 (2008) 5823–5827.
[13] Yu.I. Aristov, V.E. Sharonov, M.M. Tokarev, Universal relation between the boundary temperatures of a basic cycle of sorption heat machines, Chem. Eng. Sci. 63 (11) (2008) 2907–2912.